ISSN 0023-1584, Kinetics and Catalysis, 2006, Vol. 47, No. 4, pp. 487–496. © MAIK "Nauka/Interperiodica" (Russia), 2006.
Original Russian Text © A.M. Starik, N.S. Titova, 2006, published in Kinetika i Kataliz, 2006, Vol. 47, No. 4, pp. 504–513.

Intensification of the Oxidation of Rich Methane/Air Mixtures by O_2 Molecules Excited to the $a^1\Delta_g$ State

A. M. Starik and N. S. Titova

Central Institute of Aviation Motors, Moscow, 111116 Russia
e-mail: star@ciam.ru

Received October 18, 2004

Abstract—Methane oxidation in rich CH_4/air mixtures can be intensified by exciting O_2 molecules to the $a^1\Delta_g$ state. Even small amounts of $O_2(a^1\Delta_g)$ molecules reduce the ignition temperature and shorten the induction period. As compared to the oxidation of ordinary methane/air mixtures, oxidation in the presence of excited oxygen makes it possible to convert methane into synthesis gas (H_2 + CO) at low initial temperatures of ~600 K and atmospheric pressure and to raise the H_2 and CO yields at a fixed reactor length.

DOI: 10.1134/S0023158406040033

The oxidation of fuel-rich hydrocarbon–oxygen (air) mixtures has been the subject of numerous studies [1–7]. On the one hand, the interest in this process stems from the importance of a correct description of combustion in diffusion flames and in various combustors operating in a diffusion mode, where fuel-enriched zones always exist. On the other hand, this interest is due to the fact that the combustion of rich mixtures can be commercially used in the production of synthesis gas (CO + H_2), which is employed in the chemical and power industries. In the latter case, an important problem is to ensure the combustion of rich C_nH_m/O_2 mixtures with a fuel-to-oxidizer ratio of $\phi \geq 2$ in order to obtain high yields of H_2 and CO. Thermodynamic calculations demonstrate that raising ϕ from 2 to 3 will increase the H_2 and CO concentrations in the combustion products of the CH_4/air mixture from 16 to 28% and from 12 to 17%, respectively [8]. The H_2 concentration in the combustion products is increased by adding H_2O to the initial mixture. However, rather high pressures ($P_0 > 3$ MPa) and temperatures ($T_0 > 1200$ K) are necessary for the combustion of such rich mixtures.

It was demonstrated in earlier studies [9, 10] that introducing metastable, electronically excited, $O_2(a^1\Delta_g)$ molecules into the H_2/O_2 mixture significantly shortens the induction period and lowers the ignition limit. These effects arise from the intensification of the chain mechanism of combustion, which is primarily due to the acceleration of the chain initiation reaction $H_2 + O_2 = 2OH^{\bullet}$ by electronically excited $O_2(a^1\Delta_g)$ molecules. Note that the induction period τ_{in} can be shortened simply by heating the mixture. However, it was demonstrated in our earlier study [10] that, in terms of τ_{in}, exciting O_2 molecules is more efficient than heating the mixture by a factor of several hundreds. A considerable $O_2(a^1\Delta_g)$ concentration (~1–5%) can be achieved either by activating O_2 molecules in an electric discharge [11, 12] or by using laser radiation [10, 13].

Since dioxygen oxidizes not only H_2 but also any other hydrocarbon fuel, including methane, it is interesting to study the effects of excited O_2 molecules on the ignition temperature of rich CH_4/air mixtures and on the dynamics of H_2 formation. These effects are the subject of this publication.

KINETIC MODEL

The oxidation of rich methane/air mixtures is known to have some specific features as compared to the oxidation of stoichiometric and lean mixtures [4]. These specific features cause the maximum gas temperature and H_2O concentration at the instant of ignition of a rich CH_4/air mixture or in the flame front to exceed their equilibrium values [1–4]. Therefore, the kinetic schemes used in the simulation of the oxidation of rich mixtures should take into account these features. Rather complicated kinetic models should be used in the description of the ignition and combustion of rich methane/air mixtures even if the electronically excited molecules $O_2(a^1\Delta_g)$ and $O_2(b^1\Sigma_g^+)$ are absent from the mixture.

In this work, a reaction mechanism suggested for the space reaction between methane and O_2 or air [14] is used as the basis. This mechanism includes 433 reversible reactions involving 66 components and provides a good agreement between calculated and observed ignition delay data for stoichiometric and fuel-depleted mixtures in wide temperature and pressure ranges [14, 15]. This mechanism has been aug-

Table 1. Additional reactions included in the kinetic scheme

No.	Reaction	k_q^+, (cm^3/mol)$^{m-1}$ s^{-1}			k_q^-, (cm^3/mol)$^{m-1}$ s^{-1}			Reference
		A_q	n_q	E_{aq}	A_q	n_q	E_{aq}	
1	$CH_3^{\bullet} + H = CH_2^{\bullet} + H_2$	6.03×10^{13}	0	7589	1.32(13)	0	5629	[16]
2	$CH_3^{\bullet} + OH^{\bullet} = CH_2OH^{\bullet} + H$	2.64×10^{19}	–1.8	4038	–	–	–	[19], [20]
3	$CH_3^{\bullet} + OH^{\bullet} = CH_3O^{\bullet} + H$	5.7×10^{12}	–0.23	6900	–	–	–	[19], [20]
4	$CH_2^{\bullet} + OH^{\bullet} = CH_2O^{\bullet} + H$	2.5×10^{13}	0	0	–	–	–	[17]
5	$CH_2^{\bullet} + O_2 = CH_2O^{\bullet} + O$	4.0×10^{10}	0	0	–	–	–	[24]
6	$CH_2^{\bullet} + CO_2 = CH_2O^{\bullet} + CO$	1.0×10^{11}	0	500	–	–	–	[17]
7	$CH_2^{\bullet} + CH^{\bullet} = C_2H_2 + H$	4.0×10^{13}	0	0	–	–	–	[18]
8	$2CH_2^{\bullet} = C_2H_2 + H_2$	3.2×10^{13}	0	0	–	–	–	[18]
9	$CH_2^{\bullet} + CH_3^{\bullet} = C_2H_4 + H$	4.0×10^{13}	0	0	–	–	–	[18]
10	$CH_2^{\bullet} + C_2H_6 = CH_3^{\bullet} + C_2H_5^{\bullet}$	6.5×10^{12}	0	3855	–	–	–	[21]
11	$CH^{\bullet} + OH^{\bullet} = HCO^{\bullet} + H$	3.0×10^{13}	0	0	–	–	–	[17]
12	$CH^{\bullet} + O = CO + H$	3.97×10^{13}	0	0	–	–	–	[23]
13	$CH^{\bullet} + CH_3^{\bullet} = C_2H_3^{\bullet} + H$	3.0×10^{13}	0	0	–	–	–	[17]
14	$CH^{\bullet} + CH_4 = C_2H_4 + H$	6.0×10^{13}	0	0	–	–	–	[17]
15	$HCO^{\bullet} + HO_2^{\bullet} = CO_2 + OH^{\bullet} + H$	3.0×10^{13}	0	0	–	–	–	[22]
16	$C_2H_4 + H_2 = 2CH_3^{\bullet}$	2.34×10^{17}	0	43539	4.68×10^{15}	0	15515	[16]
17	$C_2H_4 + C_2H^{\bullet} = C_2H_3^{\bullet} + C_2H_2$	3.02×10^{13}	0	0	1.91×10^{13}	0	12148	[16]
18	$C_2H_4 + H_2 + M = C_2H_6 + M$	1.1×10^{16}	0	19123	2.29×10^{17}	0	34037	[16]
19	$C_2H_3^{\bullet} + H = 2CH_2^{\bullet}$	1.45×10^{15}	0	34278	2.0×10^{13}	0	0	[16]
20	$2CH_2^{\bullet} = C_2H_2 + 2H$	2.0×10^{14}	0	0	7.41×10^{15}	0	11618	[16]

mented with 20 reversible reactions. These reactions, together with their forward and reverse rate constants (k_q^+ and k_q^-), are presented in Table 1. The coefficients of the Arrhenius equation $k_q(T) = A_q T^{n_q} \exp(-E_{aq}/T)$ (A_q, n_q, and E_{aq}) were taken from [16–24] (E_{aq} is expressed in kelvins). If the coefficients for calculating k_q^- could not be found in the literature, their values were calculated in terms of the principle of detailed balancing using conventional relationships. The thermodynamic data necessary for the calculations were taken from [25].

In order to ascertain that the augmented mechanism is applicable to processes in rich CH_4/O_2 (air) mixtures, the calculated ignition delay times were compared with experimental data obtained with shock tubes [26, 27]. A comparison between calculated and experimental data for the $CH_4/O_2/Ar$ mixture with $\phi = 2$ at various temperatures and pressures is presented in Table 2. The induction period in numerical simulation, as in the experiment, is determined by the time necessary to reach the maximum pressure gradient. Clearly, the augmented mechanism is in satisfactory agreement with the experimental data [26, 27].

Furthermore, this mechanism accounts for the observation that the H_2O vapor concentration in the flame front in the ignition of a $\phi \geq 2$ CH_4/O_2 mixture exceeds its equilibrium value. Table 3 compares the maximum and equilibrium H_2O, H_2, CO, and CO_2 concentrations measured in the laminar flame of a $\phi = 2.13$ CH_4/O_2 mixture at $P_0 = 0.1$ MPa [1] to their calculated values. Figure 1 shows the time variation of the mole fractions of CH_4, O_2, H_2, CO, and H_2O ($\gamma_i = N_i/N$, $N = \sum_i N_i$, and N_i is the number density of the molecules of the ith component of the mixture) and temperature for the ignition of a $\phi = 2$ CH_4/air mixture at $P_0 = 0.1$ MPa and $T_0 = 1000$ K. Note that at a rather high ini-

Table 2. Experimental ignition delay data for the $CH_4/O_2/Ar$ ($\phi = 2$) mixture [26, 27] in comparison with the same data calculated using the augmented reaction mechanism

T, K	P, atm	CH_4, %	O_2, %	τ_{in}, μs	
				experimental	calculated
1680	8.52	2.12	2.12	510	537
1699	8.44	2.12	2.12	455	463
1905	10.22	2.12	2.12	95	87.9
2025	10.49	2.12	2.12	47	41.2
1658	10.56	6.7	6.7	245	179
1717	10.68	6.7	6.7	145	115
1883	13.01	6.7	6.7	45	33.6
1920	12.97	6.7	6.7	38	27.5
2000*	–	3.0	3.0	45.8	40.2

* $\rho = 6 \times 10^{-5}$ mol/cm^3.

tial gas temperature of $T_0 \geq 1500$ K, the oxidation of a rich methane/air mixture or methane pyrolysis may yield soot particles, on which heterogeneous reactions changing the concentration of active sites may take place. However, for $\phi = 2$–3 mixtures at $T_0 \leq 1200$ K (it is these regimes that are analyzed in this work), no soot is formed within the time interval $[0, \tau_{in}]$. Therefore, their effect on the formation kinetics of active sites and radicals and on the ignition dynamics is negligible. The formation of soot particles in rich methane/air mixtures at $\tau > \tau_{in}$ are beyond the scope of this study.

In order to determine the minimum set of reactions sufficient for a correct description of the ignition and heat evolution dynamics in rich CH_4/O_2 (air) mixtures in wide temperature and pressure ranges, we analyzed the reducibility of the complete kinetic scheme. It was demonstrated that the reduced mechanism that includes 215 reactions involving 34 components (H_x (x = 1, 2), O_y (y = 1–3), HO_x, H_2O_x, C, CO_x, CH_q (q = 1–4), C_2H_z (z = 1–6), CH_yO, CH_2OH, CH_3OH, CH_3O_2, CH_3O_2H, N_x, NO_x, and N_2O) leads to the same values of ignition delay, temperature, and basic component concentrations for the CH_4/air mixture as the complete scheme.

In order to study methane conversion dynamics in the CH_4/air mixture in the presence of $O_2(a^1\Delta_g)$ molecules, the above scheme should be supplemented with reactions involving $O_2(a^1\Delta_g)$ and $O_2(b^1\Sigma_g^+)$ molecules. The latter results from the interaction between $O_2(a^1\Delta_g)$ molecules: $2O_2(a^1\Delta_g) = O_2(b^1\Sigma_g^+) + O_2(X^3\Sigma_g^-)$. They can exert a certain effect on the methane oxidation kinetics. Note that electronic–electronic exchange upon collision between an excited molecule $O_2(a^1\Delta_g)$ or $O_2(b^1\Sigma_g^+)$ and an O atom in the ground electronic state (^3P) can yield an excited atom $O(^1D)$: $O_2(a^1\Delta_g, b^1\Sigma_g^+) + O(^3P) = O_2(X^3\Sigma_g^-) + O(^1D)$. These atoms are more reactive than oxygen atoms in the ground electronic state. However, according to our analysis, the quenching rate of $O(^1D)$ atoms is much higher than the rate of the chemical reactions of these atoms in the temperature and pressure ranges of interest (T_0 = 600–1200 K and $P_0 = 10^4$–10^6 Pa). For this reason, all reactions involving $O(^1D)$ atoms were left out of consideration.

The additional processes included in the scheme modified for analysis of the ignition and combustion of rich CH_4/air mixtures are presented in Table 4. The rate constants of the reactions involving $O_2(a^1\Delta_g)$ and $O_2(b^1\Sigma_g^+)$ molecules were determined by a procedure reported in our earlier work [10], using $k_q^+(T)$ and $k_q^-(T)$ data for reactions in the system H_2–$O_2(X^3\Sigma_g^-)$–$O_2(a^1\Delta_g)$–$O_2(b^1\Sigma_g^+)$–$OH^\bullet$–H_2O–$HO_2^\bullet$–H_2O_2–O_3–O–H. In particular, the rate constants of reactions 32–47, 50,

Table 3. Maximum and equilibrium component mole fractions (γ_{max} and γ_e): experimental [1] and calculated data

Component	γ_{max}		γ_e	
	experimental	calculated	experimental	calculated
H_2O	0.30	0.354	0.25	0.248
H_2	–	–	0.40	0.372
CO	–	–	0.30	0.300
CO_2	0.03	0.0263	0.02	0.0239

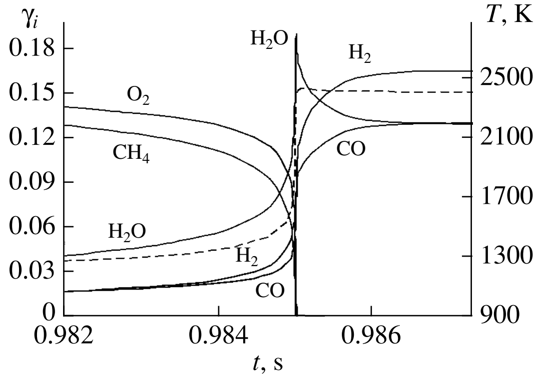

Fig. 1. Variation of the mole fractions (γ_i) of $i = CH_4$, O_2, H_2O, H_2, and CO (solid lines) and temperature (dashed line) during the space reaction between methane and air for $\phi = 2$, $T_0 = 1000$ K, and $P_0 = 10^5$ Pa.

51, 56, 57, 64–69, 72–77, 80–83, 88, and 89 were calculated using the following relationships:

$$k_q^+(T) = A_q T^{n_q} \exp(-E^e_{a,q}/T), \tag{1}$$

$$E^e_{a,q} = \frac{1}{2}\left(\sqrt{(\Delta H + E_e)^2 + 4E_a^0(\Delta H + E_a^0)} - (\Delta H + E_e)\right). \tag{2}$$

Here, A_q is a coefficient in the Arrhenius equation for the rate constant of a reaction involving the unexcited molecule, ΔH is the heat efficiency of the reaction, E_a^0 is the activation energy of the reaction involving the unexcited O_2 molecule, and E_e is the energy of the electronically excited state of the O_2 molecule (e = $a^1\Delta_g$, $b^1\Sigma_g^+$).

Note that this simple approach to the calculation of the rate constants of reactions involving the electronically excited molecules $O_2(a^1\Delta_g)$ and $O_2(b^1\Sigma_g^+)$ provides a good fit both to the experimentally determined (and recommended [28]) rate constants of the reactions H + $O_2(a^1\Delta_g)$ = $OH^\bullet$ + O and $H_2 + O_2(a^1\Delta_g) = H + HO_2^\bullet$ (nos. 3 and 9) and to the $k_q^+(T)$ data calculated for by the bond-energy-bond-order method [29] for the reactions $H_2O + O_2(a^1\Delta_g) = OH^\bullet + HO_2^\bullet$ and $CH_4 + O_2(a^1\Delta_g) = CH_3^\bullet + HO_2^\bullet$ (nos. 11 and 36). For example, the $k_q^+(T)$ values calculated for reactions 3 and 9 using relationships (1) and (2) are only twice smaller than the $k_q^+(T)$ values for $T \geq 600$ K presented in [28]. For reactions 11 and 36, the k_q^+ value (300 K $\leq T \leq$ 1000 K) calculated by formulas (1) and (2) differs from the value determined by the bond-energy-bond-order method [29] by a factor no greater than 2 and 3, respectively.

For reactions with $E_a^0 \approx 0$ in which the resulting O_2 molecule is in the ground state $X^3\Sigma_g^-$ or in the excited state $a^1\Delta_g$ or $b^1\Sigma_g^+$ (nos. 52–55, 58–61, 86, 87, 90, and 91), it was assumed that the formation rates of $O_2(X^3\Sigma_g^-)$, $O_2(a^1\Delta_g)$, and $O_2(b^1\Sigma_g^+)$ are proportional to the degeneracy of the state. In the calculation of the rate constants of the forward reactions 48, 49, 62, and 63 using formula (1), the energy barrier was increased by the energy of the electronic state $a^1\Delta_g$ or $b^1\Sigma_g^+$ ($E^e_{a,q} = E_a^0 + E_e$). The quenching rate constant data for the $a^1\Delta_g$ and $b^1\Sigma_g^+$ states of the O_2 molecule were taken from [10] for M = O, O_3, O_2, H_2, H_2O, $HO_2^\bullet$, and H_2O_2 and from [30, 31] for M = CO_2, CO, and N_2. For M = H, C, and N, it was assumed that the probability of quenching is the same as in the case of M = O; for M = CH_q, C_2H_z, CH_yO, $CH_2OH^\bullet$, CH_3OH, $CH_3O_2^\bullet$, and CH_3O_2H, the probability of quenching was taken to be the same as in the case of M = H_2O; for M = NO, NO_2, and N_2O, the same as in the case of M = N. The rate constants of the corresponding reverse reactions were calculated using the principle of detailed balancing.

IGNITION DYNAMICS OF RICH CH_4–O_2 (AIR)–$O_2(a^1\Delta_g)$ MIXTURES

For the sake of simplicity, consider methane oxidation with air containing $O_2(a^1\Delta_g)$ molecules in a closed, adiabatic, stirred reactor and assume that the gas is nonviscous and non-heat-conducting. Note that this approximation is frequently used in the kinetic analysis of the oxidation and ignition of various mixtures [32–34]. As usual, we will assume that a thermodynamic equilibrium is established between translational, rotational, and vibrational degrees of freedom. The electronically excited O_2 molecules will be treated as individual chemical components with their enthalpies of formation and heat capacities. The set of equations describing the time variation of the temperature, pressure, and composition of the reacting mixture will then include an energy conservation equation, equations for the concentrations of the species involved in chemical reactions, and an equation of state [32]. The thermodynamic data and molecular constants for unexcited components will be taken to be the same as in [14].

The ignition of C_nH_m/O_2 (air) mixtures is known to be determined by the competition between the formation of active radicals involved in chain reactions (O, H, $OH^\bullet$, $CH_3^\bullet$, and $CH_2O^\bullet$ for methane/air mixtures) and the depletion of these radicals in the reaction zone because of their diffusion or loss on the reactors walls

Table 4. Reactions involving $O_2(a^1\Delta_g)$ and $O_2(b^1\Sigma_g^+)$ molecules that are included in the kinetic scheme of methane–air combustion

No.	Reaction	No.	Reaction
1	$O_2(a^1\Delta_g) + M = 2O + M$	36	$CH_4 + O_2(a^1\Delta_g) = CH_3^{\bullet} + HO_2^{\bullet}$
2	$O_2(b^1\Sigma_g^+) + M = 2O + M$	37	$CH_4 + O_2(b^1\Sigma_g^+) = CH_3^{\bullet} + HO_2^{\bullet}$
3	$O_2(a^1\Delta_g) + H = OH^{\bullet} + O$	38	$CH_3^{\bullet} + O_2(a^1\Delta_g) = CH_3O^{\bullet} + O$
4	$O_2(b^1\Sigma_g^+) + H = OH^{\bullet} + O$	39	$CH_3^{\bullet} + O_2(b^1\Sigma_g^+) = CH_3O^{\bullet} + O$
5	$H_2 + O_2(a^1\Delta_g) = 2OH^{\bullet}$	40	$CH_3O^{\bullet} + O_2(a^1\Delta_g) = CH_2O^{\bullet} + HO_2^{\bullet}$
6	$H_2 + O_2(b^1\Sigma_g^+) = 2OH^{\bullet}$	41	$CH_3O^{\bullet} + O_2(b^1\Sigma_g^+) = CH_2O^{\bullet} + HO_2^{\bullet}$
7	$HO_2^{\bullet} + M = O_2(a^1\Delta_g) + H + M$	42	$CH_3^{\bullet} + O_2(a^1\Delta_g) = CH_2O^{\bullet} + OH^{\bullet}$
8	$HO_2^{\bullet} + M = O_2(b^1\Sigma_g^+) + H + M$	43	$CH_3^{\bullet} + O_2(b^1\Sigma_g^+) = CH_2O^{\bullet} + OH^{\bullet}$
9	$H_2 + O_2(a^1\Delta_g) = H + HO_2^{\bullet}$	44	$CO + O_2(a^1\Delta_g) = CO_2 + O$
10	$H_2 + O_2(b^1\Sigma_g^+) = H + HO_2^{\bullet}$	45	$CO + O_2(b^1\Sigma_g^+) = CO_2 + O$
11	$H_2O + O_2(a^1\Delta_g) = OH^{\bullet} + HO_2^{\bullet}$	46	$CH^{\bullet} + O_2(a^1\Delta_g) = CO + OH^{\bullet}$
12	$H_2O + O_2(b^1\Sigma_g^+) = OH^{\bullet} + HO_2^{\bullet}$	47	$CH^{\bullet} + O_2(b^1\Sigma_g^+) = CO + OH^{\bullet}$
13	$OH^{\bullet} + O_2(a^1\Delta_g) = O + HO_2^{\bullet}$	48	$HCO^{\bullet} + O = CH^{\bullet} + O_2(a^1\Delta_g)$
14	$OH^{\bullet} + O_2(b^1\Sigma_g^+) = O + HO_2^{\bullet}$	49	$HCO^{\bullet} + O = CH^{\bullet} + O_2(b^1\Sigma_g^+)$
15	$2HO_2^{\bullet} = H_2O_2 + O_2(a^1\Delta_g)$	50	$CH_2OH^{\bullet} + O_2(a^1\Delta_g) = CH_2O^{\bullet} + HO_2^{\bullet}$
16	$2HO_2^{\bullet} = H_2O_2 + O_2(b^1\Sigma_g^+)$	51	$CH_2OH^{\bullet} + O_2(b^1\Sigma_g^+) = CH_2O^{\bullet} + HO_2^{\bullet}$
17	$H_2O + O_2(a^1\Delta_g) = H_2O_2 + O$	52	$CH_3O_2^{\bullet} + OH^{\bullet} = CH_3OH + O_2(a^1\Delta_g)$
18	$H_2O + O_2(b^1\Sigma_g^+) = H_2O_2 + O$	53	$CH_3O_2^{\bullet} + OH^{\bullet} = CH_3OH + O_2(b^1\Sigma_g^+)$
19	$O_3 + M = O_2(a^1\Delta_g) + O + M$	54	$CH_3O_2^{\bullet} + CH_3O_2^{\bullet} = CH_3OH + CH_2O + O_2(a^1\Delta_g)$
20	$O_3 + M = O_2(b^1\Sigma_g^+) + O + M$	55	$CH_3O_2^{\bullet} + CH_3O_2^{\bullet} = CH_3OH + CH_2O + O_2(b^1\Sigma_g^+)$
21	$O_3 + H = OH^{\bullet} + O_2(a^1\Delta_g)$	56	$CH_3^{\bullet} + O_2(a^1\Delta_g) = CH_3O_2^{\bullet}$
22	$O_3 + H = OH^{\bullet} + O_2(b^1\Sigma_g^+)$	57	$CH_3^{\bullet} + O_2(b^1\Sigma_g^+) = CH_3O_2^{\bullet}$
23	$O_3 + O = O_2(X^3\Sigma_g^-) + O_2(a^1\Delta_g)$	58	$CH_3O_2^{\bullet} + O = CH_3O^{\bullet} + O_2(a^1\Delta_g)$
24	$O_3 + O = O_2(X^3\Sigma_g^-) + O_2(b^1\Sigma_g^+)$	59	$CH_3O_2^{\bullet} + O = CH_3O^{\bullet} + O_2(b^1\Sigma_g^+)$
25	$O_3 + OH^{\bullet} = HO_2^{\bullet} + O_2(a^1\Delta_g)$	60	$CH_3O_2^{\bullet} + HO_2^{\bullet} = CH_3O_2H + O_2(a^1\Delta_g)$
26	$O_3 + OH^{\bullet} = HO_2^{\bullet} + O_2(b^1\Sigma_g^+)$	61	$CH_3O_2^{\bullet} + HO_2^{\bullet} = CH_3O_2H + O_2(b^1\Sigma_g^+)$
27	$O_3 + HO_2^{\bullet} = OH^{\bullet} + O_2(X^3\Sigma_g^-) + O_2(a^1\Delta_g)$	62	$CH_3O_2^{\bullet} + CH_3O_2^{\bullet} = CH_3O^{\bullet} + CH_3O^{\bullet} + O_2(a^1\Delta_g)$
28	$O_3 + HO_2^{\bullet} = OH^{\bullet} + O_2(X^3\Sigma_g^-) + O_2(b^1\Sigma_g^+)$	63	$CH_3O_2^{\bullet} + CH_3O_2^{\bullet} = CH_3O^{\bullet} + CH_3O^{\bullet} + O_2(b^1\Sigma_g^+)$
29	$O_3 + O_2(a^1\Delta_g) = 2O_2(X^3\Sigma_g^-) + O$	64	$C_2H_6 + O_2(a^1\Delta_g) = C_2H_5^{\bullet} + HO_2^{\bullet}$
30	$O_3 + O_2(b^1\Sigma_g^+) = 2O_2(X^3\Sigma_g^-) + O$	65	$C_2H_6 + O_2(b^1\Sigma_g^+) = C_2H_5^{\bullet} + HO_2^{\bullet}$
31	$2O_2(a^1\Delta_g) = O_2(b^1\Sigma_g^+) + O_2$	66	$C_2H_5^{\bullet} + O_2(a^1\Delta_g) = C_2H_4 + HO_2^{\bullet}$
32	$CH_2O^{\bullet} + O_2(a^1\Delta_g) = HO_2^{\bullet} + HCO^{\bullet}$	67	$C_2H_5^{\bullet} + O_2(b^1\Sigma_g^+) = C_2H_4 + HO_2^{\bullet}$
33	$CH_2O^{\bullet} + O_2(b^1\Sigma_g^+) = HO_2^{\bullet} + HCO^{\bullet}$	68	$C_2H_4 + O_2(a^1\Delta_g) = C_2H_3^{\bullet} + HO_2^{\bullet}$
34	$HO_2^{\bullet} + CO = HCO^{\bullet} + O_2(a^1\Delta_g)$	69	$C_2H_4 + O_2(b^1\Sigma_g^+) = C_2H_3^{\bullet} + HO_2^{\bullet}$
35	$HO_2^{\bullet} + CO = HCO^{\bullet} + O_2(b^1\Sigma_g^+)$	70	$C_2H_3^{\bullet} + O_2(a^1\Delta_g) = C_2H_2 + HO_2^{\bullet}$

Table 4. (Contd.)

No.	Reaction	No.	Reaction
71	$C_2H_3^{\bullet} + O_2(b^1\Sigma_g^+) = C_2H_2 + HO_2^{\bullet}$	83	$NO + O_2(b^1\Sigma_g^+) = O + NO_2$
72	$C_2H_2 + O_2(a^1\Delta_g) = HCO^{\bullet} + HCO^{\bullet}$	84	$NO + NO + O_2(a^1\Delta_g) = NO_2 + NO_2$
73	$C_2H_2 + O_2(b^1\Sigma_g^+) = HCO^{\bullet} + HCO^{\bullet}$	85	$NO + NO + O_2(b^1\Sigma_g^+) = NO_2 + NO_2$
74	$C_2H_2 + O_2(a^1\Delta_g) = C_2H^{\bullet} + HO_2^{\bullet}$	86	$O_3 + NO = NO_2 + O_2(a^1\Delta_g)$
75	$C_2H_2 + O_2(b^1\Sigma_g^+) = C_2H^{\bullet} + HO_2^{\bullet}$	87	$O_3 + NO = NO_2 + O_2(b^1\Sigma_g^+)$
76	$C_2H^{\bullet} + O_2(a^1\Delta_g) = CO + HCO^{\bullet}$	88	$N_2 + O_2(a^1\Delta_g) = N_2O + O$
77	$C_2H^{\bullet} + O_2(b^1\Sigma_g^+) = CO + HCO^{\bullet}$	89	$N_2 + O_2(b^1\Sigma_g^+) = N_2O + O$
78	$CH_2^{\bullet} + O_2(a^1\Delta_g) = CH_2O + O$	90	$O_3 + N_2 = N_2O + O_2(a^1\Delta_g)$
79	$CH_2^{\bullet} + O_2(b^1\Sigma_g^+) = CH_2O + O$	91	$O_3 + N_2 = N_2O + O_2(b^1\Sigma_g^+)$
80	$N + O_2(a^1\Delta_g) = O + NO$	92	$O_2(a^1\Delta_g) + M = O_2(X^3\Sigma_g^-) + M$
81	$N + O_2(b^1\Sigma_g^+) = O + NO$	93	$O_2(b^1\Sigma_g^+) + M = O_2(a^1\Delta_g) + M$
82	$NO + O_2(a^1\Delta_g) = O + NO_2$		

(in small reactors) [35]. For an ignition event to take place, it is necessary that the formation time of these radicals or O or H atoms (τ_{iq}^{ch}) should be shorter than the diffusion time for the H atom (τ_D^{H}), the lightest active radical. (For a reactor with a rather large volume, the loss of active species on its walls can be neglected.) The value of τ_{iq}^{ch} determines the induction period τ_{in}. Therefore, in the first approximation, the ignition condition can be expressed as $\tau_{\mathrm{in}}(P_0, T_0) \le \tau_D^{\mathrm{H}}(P_0, T_0)$.

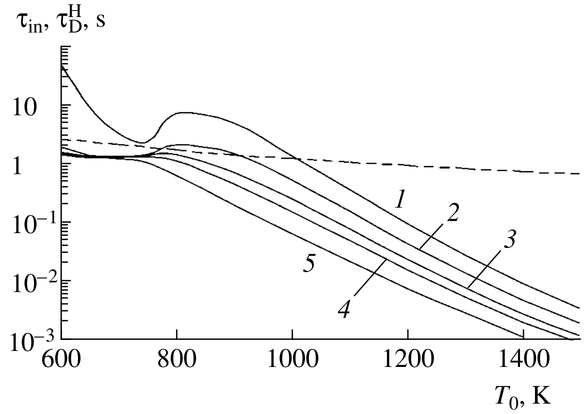

Fig. 2. $\tau_D^{\mathrm{H}}(T_0)$ (dashed line) and $\tau_{\mathrm{in}}(T_0)$ for the CH_4/air mixture ($\phi = 3$, $P_0 = 10^5$ Pa) at various $O_2(a^1\Delta_g)$ concentrations. $\gamma_{O_2(a^1\Delta_g)}$ = (*1*) 0, (*2*) 0.01, (*3*) 0.03, (*4*) 0.05, and (*5*) $0.1\gamma_{O_2}$.

Figure 2 plots the calculated dependences of the induction period and the diffusion time of H atoms on the initial temperature for the ignition of a CH_4/air mixture ($\phi = 3$, $P_0 = 10^5$ Pa) containing $O_2(a^1\Delta_g)$ in a spherical volume with $R_a = 4$ cm for various $O_2(a^1\Delta_g)$ concentrations in the mixture. Clearly, even small concentrations of $O_2(a^1\Delta_g)$ (such that its mole fraction, $\gamma_{O_2(a^1\Delta_g)}$, is 3% of the total amount of oxygen in the mixture, γ_{O_2}) cause a marked decrease in the ignition temperature T_{ign}, whose value can be determined from the relationship $\tau_{\mathrm{in}}(P_0, T_{\mathrm{ign}}) = \tau_D^{\mathrm{H}}(P_0, T_{\mathrm{ign}})$. For example, $T_{\mathrm{ign}} = 1050$ K at $\gamma_{O_2(a^1\Delta_g)} = 0$ (at the given pressure) and is as low as 550 K at $\gamma_{O_2(a^1\Delta_g)} = 0.03\gamma_{O_2}$. Furthermore, it follows from Fig. 2 that, because the $\tau_{\mathrm{in}}(T_0)$ function is nonmonotonic at lower temperatures, there can be several T_0 ranges of ignition for the CH_4/air mixture, depending on the $O_2(a^1\Delta_g)$ concentration. For $P_0 = 10^5$ Pa and $R_a = 4$ cm, ignition in the $\phi = 3$ $CH_4/O_2/N_2$ mixture at $\gamma_{O_2(a^1\Delta_g)} = 0.01\gamma_{O_2}$ will take place at $T_0 > 920$ K and $550 \text{ K} < T_0 \le 780$ K.

The decrease in τ_{in} and in the ignition temperature caused by excited O_2 molecules in the CH_4/air mixture is due to an increase in the formation rates of the $CH_3^\bullet$, $CH_2O^\bullet$, and $OH^\bullet$ radicals and O and H atoms, which are responsible for the development of the chain mechanism of methane oxidation. This point is illustrated by Fig. 3, which shows how the concentrations of the main components responsible for ignition vary with time during a space reaction in the $CH_4/O_2/N_2 = 1.5 : 1 : 3.76$ ($\phi = 3$) mixture at $T_0 = 600$ K and $P_0 = 10^5$ Pa in the absence and presence of O_2 molecules (in the latter case, $\gamma_{O_2(a^1\Delta_g)} = 0.03\gamma_{O_2}$). Clearly, even at the initial stages of the reaction ($t \approx 10^{-6}$–10^{-2} s), the abundance of $O_2(a^1\Delta_g)$ molecules causes the formation of the compounds $CH_3O^\bullet$ and $CH_3O_2^\bullet$ ($\gamma_i \sim 10^{-8}$–10^{-9}), while the amounts of $CH_3^\bullet$, $CH_2O^\bullet$, and $OH^\bullet$ active radicals and O and H atoms are considerably smaller. However, the concentration of $CH_3^\bullet$, $CH_2O^\bullet$, $OH^\bullet$, and O increase sharply to $\gamma_i \sim 10^{-4}$–10^{-8} by the point $t = 0.1$ s. This brings the mixture to a "preignition" state. However, the concentration of radicals is still insufficient for ignition. Another impact stimulating the CH_4/air mixture to ignite is provided by the recombination reactions involving the $CH_3^\bullet$ radical, namely, $2CH_3^\bullet + M = C_2H_6 + M$ and $CH_3^\bullet + O_2(a^1\Delta_g) = CH_3O_2^\bullet$, which are rather rapid at low temperatures of $T = 600$–800 K. These reactions occur with energy release. As a consequence, the gas temperature rises in the time interval $0.1 \text{ s} < t \le 1$ s, accelerating the formation of active H and O atoms and $OH^\bullet$ radicals. Raising the gas temperature causes the C_2H_6 molecule to break into methyl radicals, which further accelerate the ignition process so that the ignition event takes place at $t = 1.6$ s. If the initial mixture contains no $O_2(a^1\Delta_g)$, the formation of active radicals proceeds at a much lower rate. In this case, $\tau_{in} \approx 50$ s and $\tau_D^H \approx 3$ s; that is, the mixture does not ignite. Upon the excitation of O_2 molecules to the $O_2(a^1\Delta_g)$ state, the increase in the oxidation rate of the methane/air mixture and the shortening of the ignition time are due to an increase in the formation rates of the active radicals $CH_3^\bullet$ and $CH_2O_2^\bullet$ by the reactions $CH_4 + O_2(a^1\Delta_g) = CH_3^\bullet + HO_2^\bullet$ and $CH_3^\bullet + O_2(a^1\Delta_g) = CH_2O_2^\bullet + OH^\bullet$.

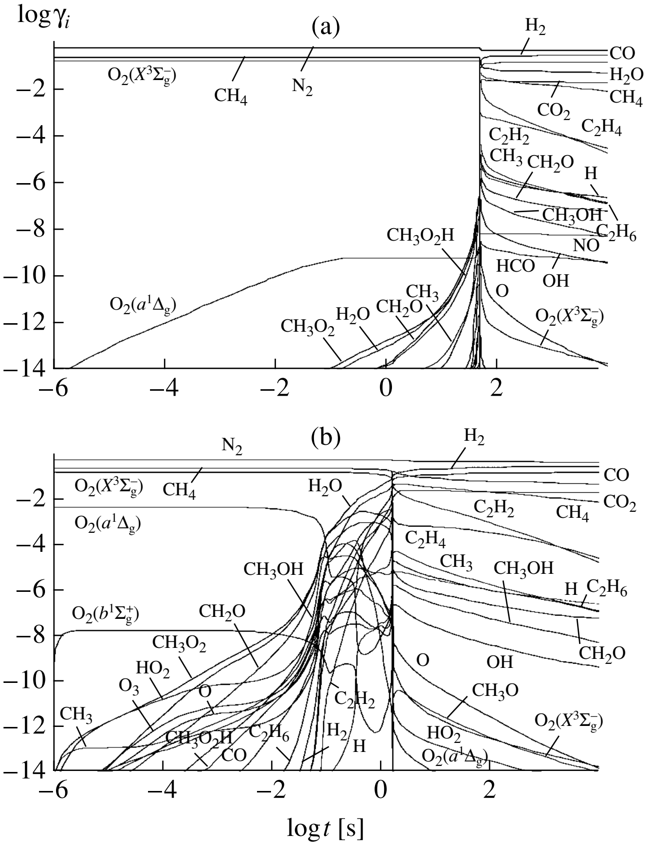

Fig. 3. Variation of the mole fractions (γ_i) of components during the space reaction in the $CH_4/O_2/N_2 = 1.5 : 1 : 3.76$ mixture ($T_0 = 600$ K, $P_0 = 10^5$ Pa) (a) in the absence of $O_2(a^1\Delta_g)$ molecules and (b) at an excited oxygen concentration of $\gamma_{O_2(a^1\Delta_g)} = 0.03\gamma_{O_2}$.

It is clear from Figs. 1 and 3 that the partial oxidation of a fuel-rich CH_4/O_2 (air) mixture includes two steps. The initial step is the formation of various radicals and ignition. In this step, considerable amounts of CH_4 and O_2 are consumed and the H_2 and CO concentrations are not high. In the second step, the H_2 and CO concentrations in the product grow rapidly, while the concentrations of CH_4 and of the hydrocarbons that have resulted from the first step of the process (C_2H_2, C_2H_4, and C_2H_6) decrease slowly. At this stage (after ignition), the gas temperature changes only slightly. Here, the formation of H_2 is mainly due to the reactions $CH_4 + H = CH_3^\bullet + H_2$, $C_2H_4 + H = C_2H_3^\bullet + H_2$, and $C_2H_6 + H = C_2H_5^\bullet + H_2$. These reactions account for 56, ~11, and ~8% of the hydrogen, respectively. The decomposition of H_2 is primarily due to the following reaction between H_2 and $OH^\bullet$: $H_2 + OH^\bullet = H_2O + H$. The formation of CO at this stage is due to the reactions $C_2H_2 + OH^\bullet = CH_3^\bullet + CO$, $HCO^\bullet + M = H + CO + M$, and $HCO^\bullet + O_2 = HO_2^\bullet + CO$, whose contributions are 58, 23.6, and 12.2%, respectively. CO decomposes by reacting with $OH^\bullet$ ($CO + OH^\bullet = H + CO_2$) and $CH_2^\bullet$ ($CH_2^\bullet + CO = C_2H_2 + O$).

Figure 4 illustrates the variation of the mole fractions of H_2 and CO forming ($\gamma_i > 0$) and disappearing ($\gamma_i < 0$) in reactions involved in the space oxidation of methane with air in the absence and presence

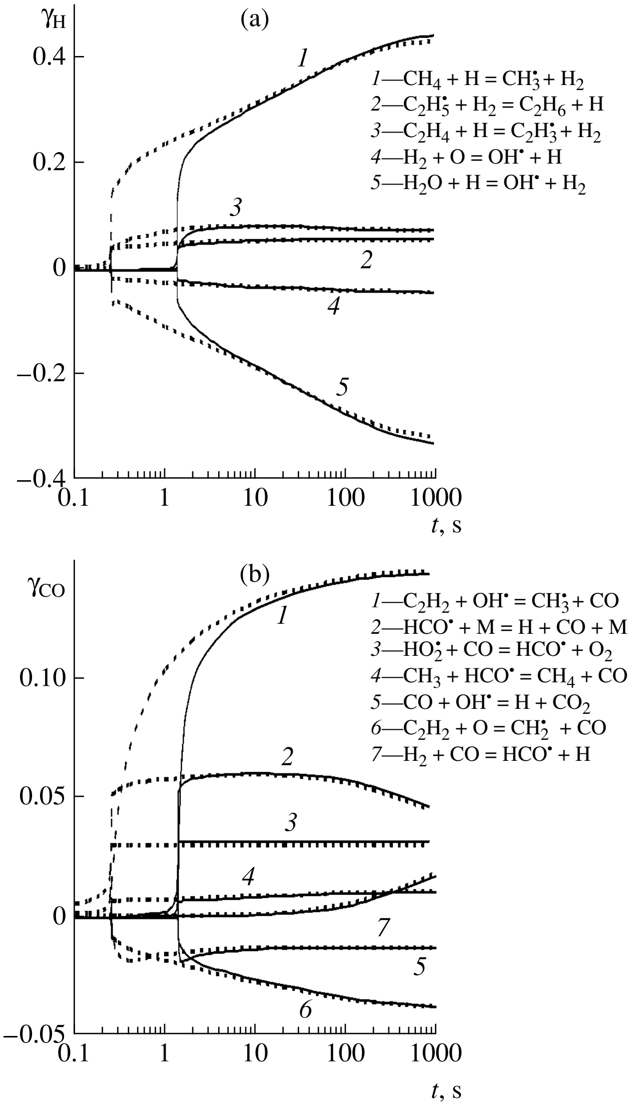

Fig. 4. Time variation of the mole fractions of (a) H_2 and (b) CO as a result of elementary reactions (a) *1–5* and (b) *1–7* in the partial oxidation of methane in the CH_4/air mixture ($\phi = 3$, $T_0 = 1000$ K, $P_0 = 10^5$ Pa) in the absence of $O_2(a^1\Delta_g)$ molecules (solid lines) and at $\gamma_{O_2(a^1\Delta_g)} = 0.03\gamma_{O_2}$ (dotted lines).

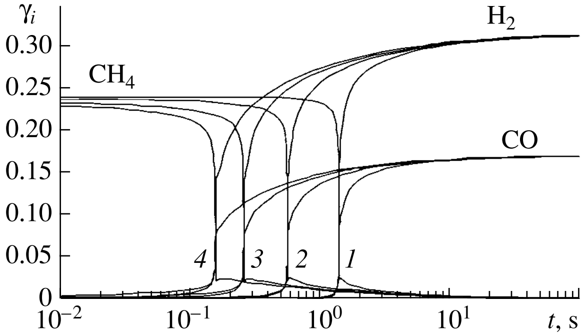

Fig. 5. Variation of the CH_4, H_2, and CO mole fractions during the space reaction in the CH_4/air mixture ($\phi = 3$, $T_0 = 1000$ K, $P_0 = 10^5$ Pa) for various initial $O_2(a^1\Delta_g)$ concentrations: $\gamma_{O_2(a^1\Delta_g)}$ = (*1*) 0, (*2*) 0.01, (*3*) 0.03, and (*4*) $0.05\gamma_{O_2}$.

($\gamma_{O_2(a^1\Delta_g)} = 0.03\gamma_{O_2}$) of $O_2(a^1\Delta_g)$ molecules for $\phi = 3$, $T_0 = 1000$ K, and $P_0 = 10^5$ Pa. The numbers in this figure are reaction numbers. The excited O_2 molecules present in the mixture does not change the contributions from the reactions yielding H_2 and CO to the amounts of these products. They change only the point in time starting at which these reactions are significant: H_2 and CO formation begins earlier in the presence of $O(a^1\Delta_g)$. This is due to a shortening of the initial stage of methane conversion in the rich CH_4/air mixture. Figure 5 shows the time profiles of the CH_4, H_2, and CO concentrations for the partial oxidation of methane in CH_4/air mixtures ($\phi = 3$, $T_0 = 1000$ K, $P_0 = 10^5$ Pa) with various $O_2(a^1\Delta_g)$ contents. Raising the concentration of $O_2(a^1\Delta_g)$ molecules in the initial methane/air mixture allows the H_2 and CO yields resulting from methane conversion to be markedly increased at a given gas residence time τ_{res} (or reactor length for a flow reactor). For example, for $\tau_{res} = 0.6$ s and $\gamma_{O_2(a^1\Delta_g)} = 0.01\gamma_{O_2}$ in the CH_4/air mixture, the H_2 and CO mole fractions at the reactor outlet are 18 and 10%, respectively. In the absence of $O_2(a^1\Delta_g)$ in the initial methane/air mixture, no methane conversion takes place at this τ_{res} value and the given gas parameters ($\phi = 3$, $T_0 = 1000$ K, and $P_0 = 10^5$ Pa). Raising the $O_2(a^1\Delta_g)$ concentration to 3% of the total O_2 content increases the outlet H_2 and CO concentrations to 25 and 13%, respectively. In order to achieve the same H_2 and CO concentrations in the conversion product without introducing $O_2(a^1\Delta_g)$, it is necessary to increase the reactor length (or τ_{res}) by a factor of 3.

Note that the intensifying effect of $O_2(a^1\Delta_g)$ on methane conversion in fuel-rich CH_4/air mixtures is both free-radical and thermal in nature. At $t \sim 0.1$ s, the energy of the excited state $a^1\Delta_g$ does not relax even at comparatively high temperatures ($T_0 \approx 1000$ K) and pressures ($P_0 \approx 10^5$ Pa). However, in the time interval $[0, \tau_{in}]$, $O_2(a^1\Delta_g)$ causes some increase in T. This is illustrated by gas temperature profiles calculated for the partial oxidation of CH_4/air mixtures ($\phi = 3$, $T_0 = 1000$ K, $P_0 = 10^5$ Pa) with various $O_2(a^1\Delta_g)$ contents (Fig. 6). As $\gamma_{O_2(a^1\Delta_g)}$ increases from 0 to 10% of the γ_{O_2} value, the gas temperature in the time interval $[0, \tau_{in}]$ rises from 1000 K (for $\gamma_{O_2(a^1\Delta_g)} = 0$) to 1200 K, further accelerating methane oxidation and shortening the

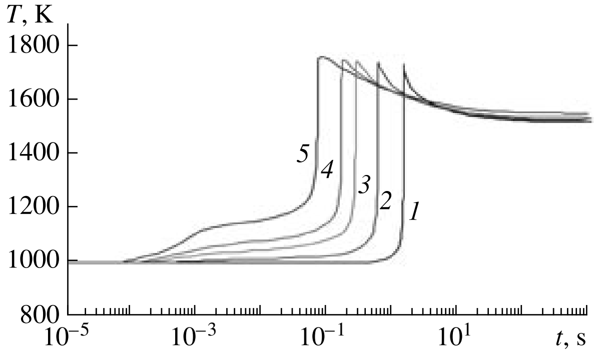

Fig. 6. Variation of temperature during the space reaction in the CH_4/air mixture ($\phi = 3$, $T_0 = 1000$ K, $P_0 = 10^5$ Pa) for various initial $O_2(a^1\Delta_g)$ concentrations: $\gamma_{O_2(a^1\Delta_g)}$ = (*1*) 0, (*2*) 0.01, (*3*) 0.03, (*4*) 0.05, and (*5*) $0.1\gamma_{O_2}$.

duration of the first stage of conversion. The temperature rise in the time interval $[0, \tau_{in}]$ is primarily due to the reactions $O_2(a^1\Delta_g) + H + M = HO_2^{\bullet} + M$ and $CH_3^{\bullet}$ + $O_2(a^1\Delta_g) = CH_3O_2^{\bullet}$. These reactions produce heat (298.1 and 212.7 kJ/mol, respectively) and are significant in the time interval examined only if $O_2(a^1\Delta_g)$ molecules are present in the initial mixture.

CONCLUSIONS

The excitation of O_2 molecules to the $a^1\Delta_g$ state intensifies oxidation in fuel-rich methane/air mixtures. This effect is due to the fact that chain reactions with $O_2(a^1\Delta_g)$ molecules in place of ordinary dioxygen proceed at a higher rate and is unrelated to the heating of the gas due to the quenching of the excited states $O_2(a^1\Delta_g)$ and $O_2(b^1\Sigma_g^+)$. This makes it possible to substantially decrease the ignition limit for the fuel-rich CH_4/air mixture and to convert methane into synthesis gas ($H_2 + CO$) at comparatively low initial temperatures (~600 K) and atmospheric pressure. As compared to the partial oxidation of an ordinary methane/air mixture containing no excited oxygen molecules, the same process in the presence of $O_2(a^1\Delta_g)$ molecules, even if their proportion is as small as ~3% of the total O_2 concentration, are characterized by a markedly shorter induction period and methane oxidation time and affords higher H_2 and CO yields at a given gas residence time.

ACKNOWLEDGMENTS

This study was supported by the Russian Foundation for Basic Research (project nos. 05-01-00355 02-02-81016, and 04-02-39023) and by INTAS (grant no. 03-51-4736).

REFERENCES

1. Goodings, J.M., Bohme, K.D., and Sugden, T.M., *Sixteenth Int. Symp. on Combustion,* Pittsburgh, 1977, p. 891.
2. Milton, B.E. and Keck, J.C., *Combust. Flame*, 1984, vol. 58, no. 1, p. 13.
3. Refael, S. and Sher, E., *Combust. Flame*, 1989, vol. 78, nos. 3–4, p. 326.
4. Lui, F., Guo, H., Smallwood, G., and Gulder, O., *29th Int. Symp. on Combustion,* Pittsburgh, 2002, p. 12.
5. Zamanshchikov, V.V., Namyatov, I.G., Bunev, V.A., and Babkin, V.S., *Fiz. Goreniya Vzryva*, 2004, vol. 40, no. 1, p. 38.
6. Makita, T., Yamamoto, T., Furuhata, T., and Arai, N., *J. Propul. Power*, 2003, vol. 19, no. 2, p. 226.
7. Rusanov, V.D., Bararitskii, A.I., Gerasimov, E.N., et al., *Dokl. Akad. Nauk*, 2003, vol. 389, no. 3, p. 324.
8. Borisov, A.A., Karpov, V.P., Politenkova, G.G., et al., in *Combustion and Atmospheric Pollution*, Roy, G.D., Frolov, S.M., and Starik, A.M., Eds., Moscow: Torus, 2003, p. 78.
9. Starik, A.M. and Titova, N.S., *Khim. Fiz.*, 2001, vol. 20, no. 5, p. 17.
10. Starik, A.M. and Titova, N.S., *Kinet. Katal.*, 2003, vol. 44, no. 1, p. 35 [*Kinet. Catal.* (Engl. Transl.), vol. 44, no. 1, p. 28].
11. Zakharov, A.I., Klopovskii, K.S., Osipov, A.P., et al., *Fiz. Plazmy*, 1988, vol. 14, no. 3, p. 327.
12. Schmiedberger, J. and Fujii, H., *Appl. Phys. Lett.,* 2001, vol. 78, no. 18, p. 2649.
13. Eisenberg, W.S., Shelson, A., Bulter, R., and Taylor, K., *J. Photochem.,* 1984, vol. 25, no. 2, p. 439.
14. Dautov, N.G. and Starik, A.M., *Kinet. Katal.,* 1997, vol. 38, no. 2, p. 207 [*Kinet. Catal.* (Engl. Transl.), vol. 38, no. 2, p. 185].
15. Gurentsov, E.V., Divakov, O.G., and Eremin, A.V., *Teplofiz. Vys. Temp.*, 2002, vol. 40, no. 3, p. 416 [*High Temp.* (Engl. Transl.), vol. 40, no. 3, p. 379].
16. Zhil'tsova, I.V., Zaslonko, I.S., Karasevich, Yu.K., and Vagner, Kh.G., *Kinet. Katal.*, 2000, vol. 41, no. 1, p. 87 [*Kinet. Catal.* (Engl. Transl.), vol. 41, no. 1, p. 76].
17. Leung, K.M. and Lindstedt, R.P., *Combust. Flame*, 1995, vol. 102, no. 1/2, p. 129.
18. Wang, H. and Frenklach, M., *Combust. Flame*, 1997, vol. 110, no. 1/2, p. 173.
19. Tereza, A.M., Slutskii, V.G., and Severin, E.S., *Khim. Fiz.*, 2003, vol. 22, no. 6, p. 30.
20. Dean, A.M. and Westmoreland, P.R., *Int. J. Chem. Kinet.*, 1987, vol. 19, p. 207.
21. Bohland, T., Dobe, S., Temps, F., and Wagner, H.Gg., *Ber. Bunsen-Ges. Phys. Chem.*, 1985, vol. 89, p. 1110.
22. Tsang, W. and Hampson, R.F., *J. Phys. Chem. Ref. Data*, 1986, vol. 15, no. 3, p. 1087.
23. Baulch, D.L., Cobos, C.J., Cox, R.A., et al., *J. Phys. Chem. Ref. Data*, 1994, vol. 23, no. 6, p. 847.

24. Dombrowsky, Ch., Hwang, S.M., Rohrig, M., and Wagner, H.Gg., *Ber. Bunsen-Ges. Phys. Chem.*, 1992, vol. 96, p. 194.
25. Gurvich, L.V., Khachkuruzov, G.A., Medvedev, V.A., et al., *Termodinamicheskie svoistva individual'nykh veshchestv* (Thermodynamic Properties of Individual Substances), Glushko, V.P., Ed., Moscow: Nauka, 1978.
26. Lifshitz, A., Scheller, K., Burcat, A., and Skinner, G.B., *Combust. Flame*, 1971, vol. 16, no. 3, p. 311.
27. Frenklach, M. and Bornside, D.E., *Combust. Flame,* 1984, vol. 56, no. 1, p. 1.
28. Basevich, V.Ya. and Belyaev, A.A., *Khim. Fiz.,* 1989, vol. 8, no. 8, p. 1124.
29. Mayer, S.W. and Schieler, L., *J. Phys. Chem.*, 1968, vol. 72, no. 7, p. 2628.
30. Didyukov, A.I., Kulagin, Yu.A., Shelepin, L.A., and Yarygina, V.N., *Kvantovaya Elektron.*, 1989, vol. 16, no. 5, p. 892.
31. McEven, M. and Phillips, L., *Chemistry of the Atmosphere*, London: Arnold, 1975.
32. *Combustion Chemistry*, Gardiner, W.C., Ed., New York: Springer, 1984.
33. Frenclach, M., Wang, H., and Radinowitz, M., *Prog. Energy Combust. Sci.*, 1992, vol. 15, no. 3, p. 47.
34. Kojima, S., *Combust. Flame,* 1994, vol. 99, no. 1, p. 87.
35. Zel'dovich, Ya.B., Barenblatt, G.I., Librovich, V.B., and Makhviladze, G.M., *Matematicheskaya teoriya goreniya i vzryva* (Mathematical Theory of Combustion and Explosion), Moscow: Nauka, 1980.